Vol 17 No 7, July 2008
1674-1056/2008/17(07)/2627-06

Chinese Physics B

© 2008 Chin. Phys. Soc.
and IOP Publishing Ltd

Power dissipation characteristics of great power and super high speed semiconductor switch*

Liang Lin(梁 琳), Yu Yue-Hui(余岳辉)†, and Peng Ya-Bin(彭亚斌)

Department of Electronic Science & Technology, Huazhong University of Science & Technology, Wuhan 430074, *China*

(Received 12 December 2007; revised manuscript received 8 January 2008)

The power dissipation characteristics of pulsed power switch reversely switched dynistors (RSDs) are investigated in this paper. According to the expressions of voltage on RSD, derived from the plasma bipolar drift model and the RLC circuit equations of RSD main loop, the simulation waveforms of current and voltage on RSD are acquired through iterative calculation by using the fourth order Runge–Kutta method, then the curve of transient power on RSD versus time is obtained. The result shows that the total dissipation on RSD is trivial compared with the pulse discharge energy and the commutation dissipation can be nearly ignored compared with the quasi-static dissipation. These characteristics can make the repetitive frequency of RSD increase largely. The experimental results prove the validity of simulation calculations. The influence factors on power dissipation are discussed. The power dissipation increases with the increase of the peak current and the n-base width and with the decrease of n-base doping concentration. In order to keep a low power dissipation, it is suggested that the n-base width should be smaller than 320μm when doping concentration is 1.0×10^{14}cm^{-3} while the doping concentration should be higher than 5.8×10^{13}cm^{-3} when n-base width is 270μm.

Keywords: reversely switched dynistor (RSD), pulsed power, switch, power dissipation
PACC: 6185, 7230, 8160C

1. Introduction

Pulsed power technology has been widely applied to the military and industrial areas, such as the inertial confinement fusion, electromagnetic launch, accelerator, modifying material properties, desulfurization and denitration, food freshness preservation, etc.[1−4] Pulsed power switch is one of the most important elements in a pulsed power system. Semiconductor devices can overcome the defects, such as short lifetime and instability, in traditional gas switches. Therefore, pulsed power switches tend to turn into semiconductor devices.[5−7] The ideal pulsed power switches are required to have the characteristics of high voltage, great current, high speed, low dissipation and long lifetime, etc. Low dissipation has great significance for prolonging the device lifetime. What is more, it is a necessary condition of increasing the utmost frequency at which the device operates in a repetitive mode.

The great power and superhigh speed semiconductor switch, the reversely switched dynistor (RSD), is a kind of new pulsed power discharge switch developed by Grekhov of the Ioffe Physicotechnical Institute of Russian Academy of Sciences.[8] It is based on the controllable plasma layer to carry out the current commutation.[9,10] RSDs can turn on upon the whole chip area simultaneously and uniformly because of its special structure and operation principle. The forward voltage drop has just a very little jump at the front of the pulse, and the quasi-static state appears within several microseconds (It takes about a hundred microseconds for this process in common thyristor to take place). That is to say, the total dissipation is trivial during the operation of RSD and the current commutation dissipation just occupies a small part of it. These characteristics of RSD can make it applied to the pulsed power area of repetitive frequency and high amplitude.

The power dissipation characteristics of an RSD have been analysed in this paper. Based on the plasma bipolar drift model, the current commutation dissipation and the quasi-static dissipation are calculated, separately. The relationships among peak current, structure parameters of device and power dissipation are discussed. The calculation results are affirmed by

*Project supported by the National Natural Science Foundation of China (Grant Nos 50277016 and 50577028), and supported by the Specialized Research Fund for the Doctoral Program of Higher Education of China (Grant No 20050487044).
†Corresponding author. E-mail: yuyuehui@mail.hust.edu.cn

experiments.

2. Operation principle

RSD is a thyristor-type semiconductor device with p^+-n-p-n^+ four-layer structure as shown in Fig.1. Unlike thyristor, it is a two electrode device without the gate. It contains several thousands of alternating thyristor units and transistor units in structure. The characteristic size of each unit is smaller than the width of n-base. The collector junction J_2 common to all sections blocks the external forward voltage. The junction J_3 at cathode is also in common, which is formed by the heavily doped n^+ layer ($\sim 10^{20}\mathrm{cm}^{-3}$) at cathode and the less heavily doped p layer ($\sim 10^{17}\mathrm{cm}^{-3}$).[8,11]

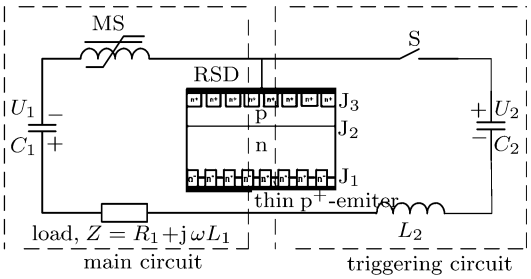


Fig.1. RSD structure and operation principle.

According to the principle of current commutation by the controllable plasma layer, the RSD turns on in the quasi diode mode after triggering. Figure 1 shows its operating external circuit, which consists of a triggering circuit and a main circuit. The two sections are separated by the saturable core choke MS.

The turn-on process of RSD is the conductance modulation process in n-base. The plasma distribution in the turn-on process in n-base is shown in Fig.2. Figure 2(a) shows the triggering process. The triggering switch S is closed at the moment t=0. The reverse triggering voltage is applied to the RSD and the MS is not saturated. The low voltage junction n^+p of transistor unit breaks down and the triggering current $J_R(t)$ flows through the embedded pnn$^+$ diode structure. The holes in p-base are injected into the n-base through the forward biased collector junction J_2. Accordingly, the electrons flow from the n^+ area to the n-base. As a result, a thin plasma layer P_1 of high concentration is formed in the n-base near the collector junction. The holes in P_1 layer drift towards the n^+ area. The front ξ_r of reversible plasma wave P_r reaches the n^+ area at the moment $t = t_1$ and the second plasma layer P_2 begins to form. The triggering current pulse usually lasts about 2μs. About 75% plasma concentrates in the layer P_1 layer near the collector in this process.

Figure 2(b) shows the turn-on process. The MS is saturated at the moment $t = t_R$. The main circuit voltage U_1 is applied to the RSD and the thyristor units start to turn on. The holes are injected from the layer P_1 into the p-base, which leads to the opposite injection of the electrons in the n^+-emitter at cathode. At the same time, the reversible wave P_r starts to return. The holes are injected from p^+-emitter at anode into plasma layer P_2 and the direct bipolar plasma wave P_f moves towards the collector J_2. The boundary ξ_f between the direct wave P_f and reversible wave P_r reaches P_1 at the moment $t = t_2$. The plasma layer P_1 is almost not depleted in this process. RSD turns on and a great forward current $J_F(t)$ flows through it.

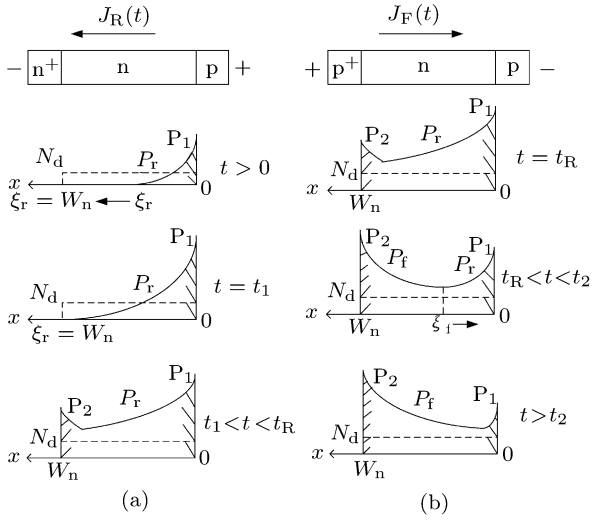


Fig.2. Plasma distribution in RSD operation process: (a) Triggering process, (b) Turn-on process.

3. Calculation of power dissipation on RSD

An x axis is set up as shown in Fig.2 with its origin located at the junction J_2. Because the transit time of electrons and holes in the n-base are on the order of several tens of nanoseconds while the carrier lifetime is usually from several microseconds to several tens of microseconds, the recombination action can be ignored. The equation describing the plasma bipolar

drift is as follows:

$$\frac{\partial p}{\partial t} = -\frac{bN_{\rm d}J(t)}{q[(b+1)p+bN_{\rm d}]^2}\frac{\partial p}{\partial x}, \tag{1}$$

where $p(x,t)$ is the excess plasma density, $N_{\rm d}$ is the n-base doping concentration, b=$\mu_{\rm n}/\mu_{\rm p}$ is the electron-to-holes mobility ratio in a weak field, and $J(t)$ is plasma current density.

The expression of $p(x,t)$ can be acquired from Eq.(1) under certain initial and boundary conditions, then the conductance and the electrical field distribution in n-base are confirmed. Finally, the expressions of voltage on RSD are obtained as follows.[8,12]

In the triggering process, we have

$$u_{\rm RSD} = \frac{W_{\rm n}^2 J_{\rm R}(t)}{\mu_{\rm p}}\left[(bQ_{\rm N})^{-1} - \frac{1}{3}Q(t)(bQ_{\rm N})^{-2}\right], \quad 0<t<t_1, \tag{2}$$

$$u_{\rm RSD} = \frac{2W_{\rm n}^2 J_{\rm R}(t)}{3\mu_{\rm p}\sqrt{bQ_{\rm N}Q(t)}}, \quad t_1 \le t < t_{\rm R}, \tag{3}$$

where $W_{\rm n}$ is the n-base width, $Q_{\rm N}$ is the donor charge surface density in the n-base, $Q_{\rm N}$=$qN_{\rm d}W_{\rm n}$, and $Q(t)=\int_0^t J_{\rm R}(t){\rm d}t$.

In the turn-on process, we have

$$u_{\rm RSD} = \frac{2W_{\rm n}^2 J_{\rm F}(t)}{3\mu_{\rm p}\sqrt{bQ_{\rm N}Q_{\rm R}}}, \quad t_{\rm R} \le t < t_2, \tag{4}$$

$$u_{\rm RSD} = \frac{2W_{\rm n}^2 J_{\rm F}(t)}{3\mu_{\rm p}\sqrt{bQ_{\rm N}Q_{\rm F}(t)}}, \quad t \ge t_2, \tag{5}$$

where $Q_{\rm R}=\int_0^{t_{\rm R}} J_{\rm R}(t){\rm d}t$, and $Q_{\rm F}(t)=\int_{t_{\rm R}}^t J_{\rm F}(t){\rm d}t$.

The following equations hold true both in the triggering circuit and in the main circuit:

$$u_{\rm L} = L\frac{{\rm d}i}{{\rm d}t}, \tag{6}$$

$$i = C\frac{{\rm d}u_{\rm C}}{{\rm d}t}, \tag{7}$$

$$u_{\rm C} = u_{\rm L} + {\rm i}R + u_{\rm RSD}(i). \tag{8}$$

The fourth order Runge–Kutta method is used to discretize the current i and voltage $u_{\rm C}$, yielding

$$i(k+1) = i(k) + \frac{u_{\rm C}(k) - i(k)R - u_{\rm RSD}(i(k))}{L}{\rm d}t, \tag{9}$$

$$u_{\rm C}(k+1) = u_{\rm C}(k) - \frac{i(k)}{C}{\rm d}t. \tag{10}$$

The initial conditions of triggering process are $u_{\rm C}(0)$=U_2 and $i(0)$=0. The initial conditions of turn-on process are $u_{\rm C}(0)$=U_1, $i(0)$=0 and $Q_{\rm R}=\int_0^{t_{\rm R}} J_{\rm R}(t){\rm d}t$. With the parameters of RSD device, the result of the iterative calculating of Eqs.(2)–(5), (9) and (10) is the simulation result for the real circuit.

The product of voltage on RSD $u_{\rm RSD}$ and current through RSD $i_{\rm RSD}$ at a corresponding time is its instantaneous power. The integration of the power in a certain period is the dissipation on the device. According to the analysis on the RSD turn-on process above, the power dissipation contains triggering dissipation and turn-on dissipation. Because the amplitude of triggering current is small and the forward voltage drop of the embedded triggering diode is very low in the effect of conductance modulation, the influence of this part is not significant. The turn-on dissipation can be divided into two parts, i.e. the current commutation dissipation at the front edge of pulse and the quasi-static dissipation.

When $t_R \le t < t_2$, the reversible wave $P_{\rm r}$ returns and the conductance modulation effect is reduced. The direct wave $P_{\rm f}$ occupies the space remaining behind by the reversible wave and contributes to the modulation of conductance. The effects of $P_{\rm r}$ and $P_{\rm f}$ cancel out, so it can be considered that the conductance in n-base keeps constant and $u_{\rm RSD}$ increases as $J_{\rm F}(t)$ increases. The RSD accomplishes the turn-on transient process in this period and the dissipation is the current commutation dissipation. When $t \ge t_2$, the direct wave $P_{\rm f}$ modulates the conductance in the n-base. The conductance increases sharply in the extremely high-level injection, which makes $u_{\rm RSD}$ decrease as a whole. The RSD is on-state in this period and the dissipation is the on-state dissipation or it is called quasi-static dissipation. Therefore, at the moment $t=t_2$ when the direct wave $P_{\rm f}$ reaches layer $\rm P_1$ the forward voltage drop on RSD has its largest value $U_{\rm Fmax}$. In the same current class, the lower the $U_{\rm Fmax}$ is, the smaller the power dissipation is.

4. Results and discussion

RSD chips of 40mm in diameter are made in our laboratory, and of them seven chips are selected out and construct a stack. The structure parameters of the device are $W_{\rm n}$=270μm and the substrate resistivity ρ=65Ω·cm. It is turned on the test platform. The main voltages are 4000 and 6000V, separately. Other external circuit parameters are as follow: C_1 =600μf, L_1=1.3μH, R_1=0.113Ω, C_2=1.18μf, L_2=0.7μH, R_2=0.08Ω, and U_2=1500V. Here the subscript 1 denotes the main circuit and subscript 2 refers

to the triggering circuit.

Figure 3 shows the current, voltage and power simulation waveforms from the RSD. Here the values of u_{RSD} and P_{RSD} are for the stack, which are seven times those of a chip correspondingly. Figure 4 shows the experimental waveforms of current and voltage. The oscillograph type is TDS1012. The current is measured by using Rogowski coil. Its proportion coefficient is 10900A/V. Figure 5 shows the power waveforms obtained from the product of corresponding values of current and voltage taken from the obtained waveforms of current and voltage.

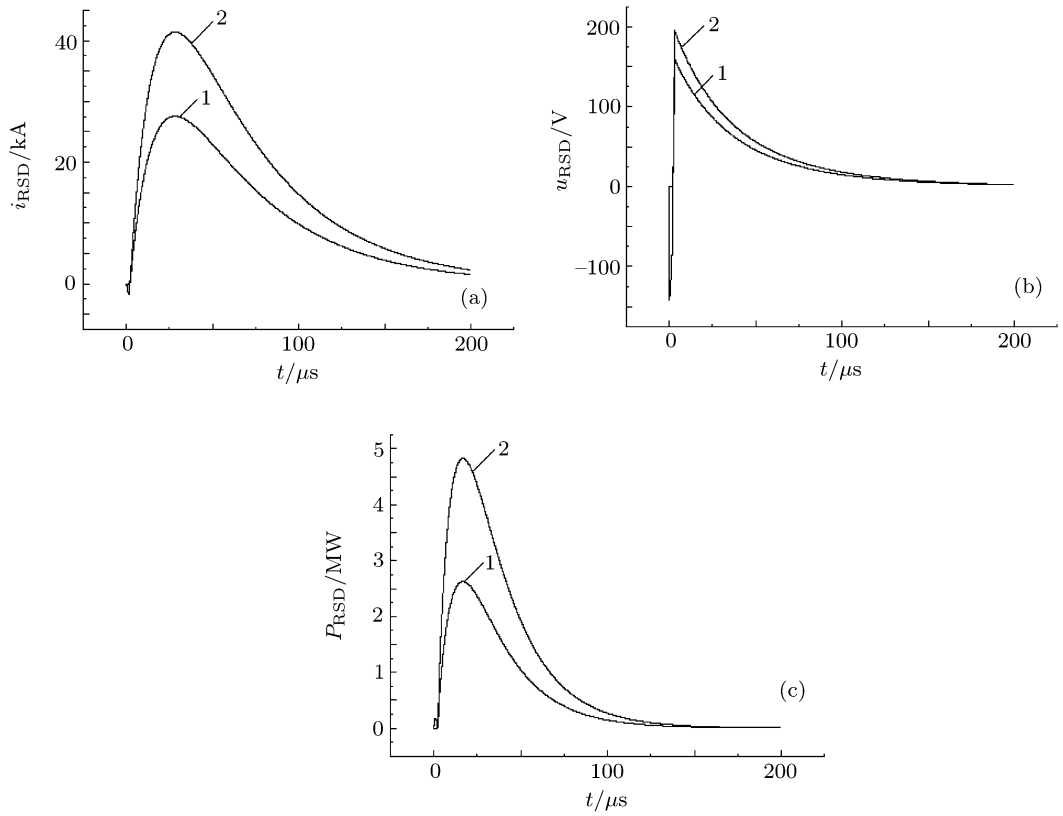


Fig.3. Simulation waveforms at main voltages of 4000V (1) and 6000V (2) showing current simulation waveforms (a), voltage simulation waveforms (b), and power simulation waveforms (c).

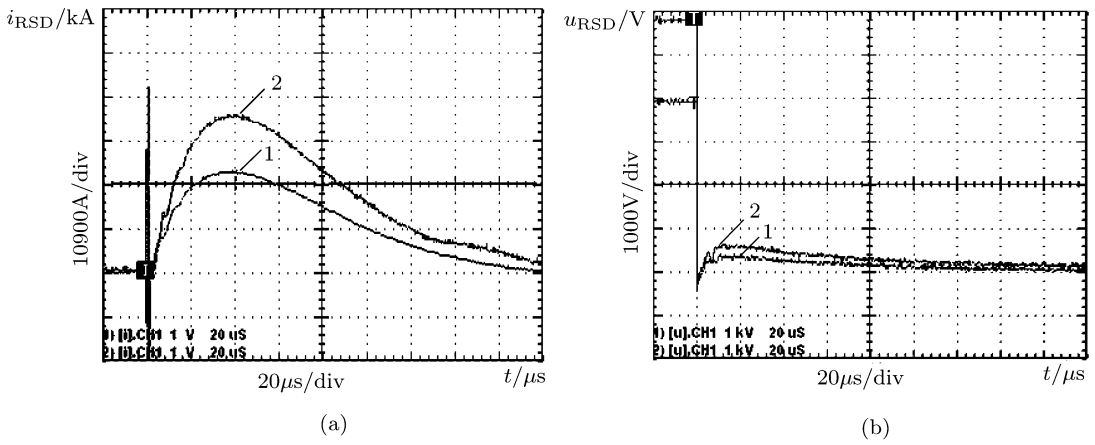


Fig.4. Experimental waveforms at main voltages of 4000V (1) and 6000V (2), showing experimental current experimental waveforms (a) and experimental voltage waveforms (b).

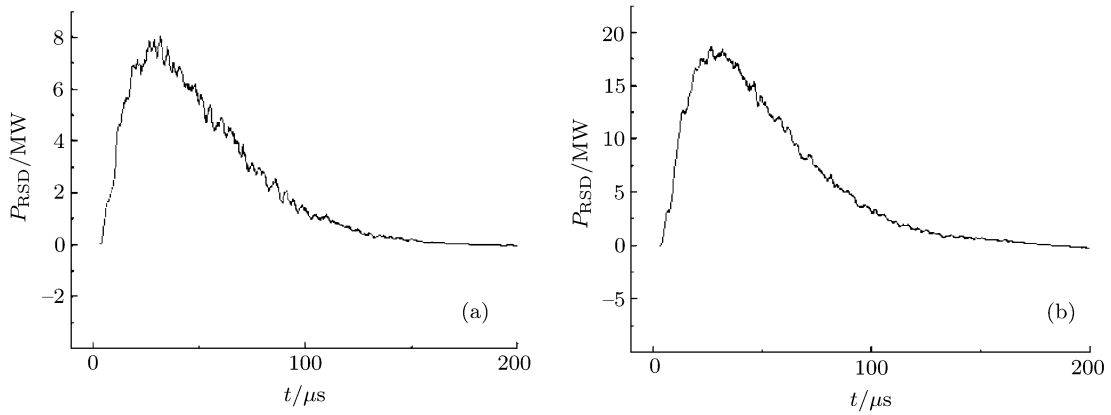


Fig.5. Power waveforms obtained from experimental results at main voltages of U_1=4000V (a) and U_1=6000V (b).

A comparison between the simulation result and the experimental result shows that the current waveforms accord well with each other in peak value, pulse width and rise rate. The simulation values of voltage and power are smaller than the experimental ones, which is caused by the voltage measurement. The voltage signal is not obtained directly at RSD chips, thereby includes the voltage drop on the packaging lead.

For the case U_1=4000V, the quasi-static state comes into being after the turn-on process has proceeded for 1.32μs, indicated by calculation, i.e. $t_2 = t_R$+1.32μs. The triggering time is set to be 2μs. In one discharge period, the triggering dissipation is 0.036J, the current commutation dissipation is 0.039J and the quasi-static dissipation is 16.471J on a single chip. They are 0.22%, 0.24% and 99.54% of the total dissipation on the RSD, respectively. The total dissipation of the pulse discharge is 4800J, of which 2.45% dissipates on the RSD stack. These results show that the dissipation on the RSD switch is trivial and the dynamic dissipation of current commutation accounts for only a small part of it. Therefore, the RSD is an ideal pulsed power switch and its operation frequency can be increased largely.

Figure 6 shows the maximum of turn-on voltage U_{Fmax} and the energy dissipation E on an RSD chip in one period versus the peak current I_m separately. As I_m increases, both U_{Fmax} and E increase. When I_m increases from 13.8 to 69.0kA, U_{Fmax} increases from 15.7 to 36.4V and E increases from 6.0 to 66.5J. Figure 7 shows the maximum of power on the RSD $(P_{RSD})_{max}$ versus n-base width W_n and doping concentration N_d separately. $(P_{RSD})_{max}$ increases as W_n increases and N_d decreases. The above results accord with the rules described by expressions (2)–(5). When N_d=1.0×10^{14}cm^{-3} and W_n increases from 220 to 520μm, $(P_{RSD})_{max}$ increases from 277 to 993kW. W_n is usually smaller than 320μm in experiment in order to keep a low dissipation. When W_n=270μm and N_d decreases from 5.0×10^{14} to 2.0×10^{13}cm^{-3}, $(P_{RSD})_{max}$ increases from 169 to 833kW. N_d is usually higher than 5.8×10^{13}cm^{-3}(80Ω·cm^{-1}) in experiment.

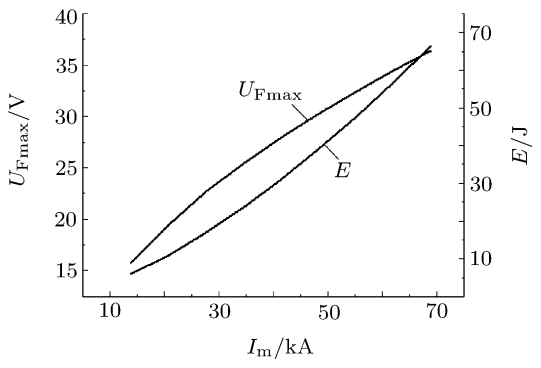


Fig.6. Maximum of turn-on voltage and energy dissipation versus peak current separately.

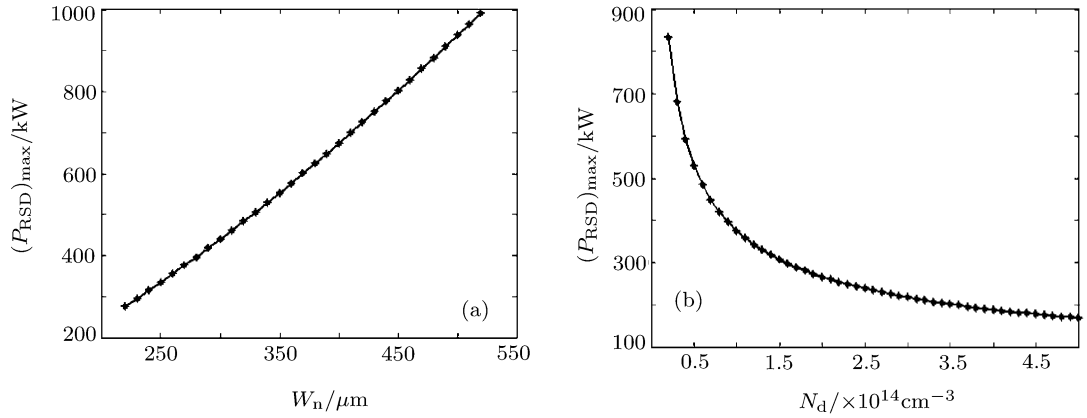


Fig.7. Maximum of power versus n-base width and doping concentration at different n-base widths (a) and different n-base doping concentrations (b) respectively.

5. Conclusion

With the iterative calculations of current and voltage relationships on RSD and RLC loop equations, the curve of power on RSD versus time is obtained. The triggering dissipation, the commutation dissipation and the quasi-static dissipation on RSD occupy 0.22%, 0.24% and 99.54% of the total dissipation, respectively. The total dissipation on RSD occupies 2.45% of the pulsed discharge energy. These characteristics can make RSD applied to the pulsed power area of repetitive frequency and high amplitude.

The influence factors on RSD power dissipation contain peak current, n-base width and doping concentration. In order to keep a low dissipation, the n-base width is usually smaller than 320μm when doping concentration is 1.0×10^{14}cm^{-3} and doping concentration is usually higher than 5.8×10^{13}cm^{-3} when the n-base width is 270μm.

Studying the power dissipation characteristics on RSD is of great significance for prolonging the lifetime and enhancing the reliability of device. Additional study should be made on measuring the value of voltage on RSD accurately.

References

[1] Sundararajan R, Jin S, Soundarajan E, Gonzales J and Chaney A 2004 *IEEE Trans. Plasma Sci.* **32** 2017
[2] Shao T, Sun G S, Yan P, Wang J, Yuan W Q and Zhang S C 2007 *Chin. Phys.* **16** 778
[3] Wang Z, Xu R K, Yang J L, Hua X S, Li L B, Xu Z P, Ning J M and Song F J 2007 *Chin. Phys.* **16** 773
[4] Gaudet J A, Barker R J, Buchenauer C J, Christodoulou C, Dickens J, Gundersen M A, Joshi R P, Krompholz H G, Kolb J F, Kuthi A, Laroussi M, Neuber A, Nunnally W, Schamiloglu E, Schoenbach K H, Tyo J S and Vidmar R J 2004 *Proc. IEEE* **92** 1144
[5] Glidden S C and Sanders H D 2006 *The Institute of Engineering and Technology Pulsed Power Symposium* p36
[6] Fazio M V and Kirbie H C 2004 *Proc. IEEE* **92** 1197
[7] Jang W H, Yatsui K, Takayama K, Akemoto M, Nakamura E, Shimizu N, Tokuchi A, Rukin S, Tarasenko V and Panchenko A 2004 *Proc. IEEE* **92** 1180
[8] Grekhov I V 1988 *Solid-State Electronics* **31** 1483
[9] Korotkov S V 2002 *Instruments and Experimental Techniques* **45** 437
[10] Aristov Y, Voronkov V, Grekhov I V, Zhmodikov A, Kozlov A, Korotkov S and Rol'nik I 2007 *Instruments and Experimental Techniques* **50** 228
[11] Yu Y H, Liang L, Li M T, Liu Y H and Liu L 2005 *Transactions of China Electrotechnical Society* **20** 36 (in Chinese)
[12] Du R F, Yu Y H, Peng Z L, Li H Y and Hu Q 2004 *Microelectron.(China)* **34** 195 (in Chinese)